RESEARCH ARTICLE

International Journal of Agriculture, Environment and Food Sciences 2024; 8(2): 261-272
DOI: https://doi.org/10.31015/jaefs.2024.2.3

Production of a novel biodegradable film made from chitosan and pomegranate (*Punica granatum* L.) seed essential oil

Murat EVCIL[1]

[1] Dicle University, Science Faculty, Department of Chemistry, 21280 Diyarbakır, Turkiye

Abstract

This study evaluated the effects of pomegranate (*Punica granatum* L.) seed essential oil (PSO) on chitosan-based films. The results showed that the addition of PSO slightly increased thickness, while significantly decreasing the moisture content, and solubility properties. The color values of the composite films containing PSO changed noticeably, with a tendency toward light brown, which was beneficial in resisting food decomposition caused by ultraviolet light. X-Ray diffraction analysis (XRD) and Fourier-transform Infrared (FT-IR) results indicated that the addition of PSO affected the structure of the chitosan films, while the interaction between chitosan and polyphenols in PSO established new hydrogen bonds. Scanning electron microscopy (SEM) showed that the surface of the PSO-containing blend films was rougher compared to the chitosan control film, and the roughness increased as the PSO content in the blend films increased. Additionally, composite films that contained PSO had substantial antibacterial action, particularly against pathogenic *E. coli*. In short, the novel active chitosan-based films with incorporated PSO present broad application prospects in the packaging of fresh-cut meat or vegetables. Therefore, this study will also be beneficial in these areas.

Keywords: Chitosan film, Pomegranate seed essential oil, Edible film, Antimicrobial, Blend films

Type: Research Article

Subject: Food Biotechnology

Citation: Evcil, M. (2024). Production of a novel biodegradable film made from chitosan and pomegranate (*Punica granatum* L.) seed essential oil. International Journal of Agriculture, Environment and Food Sciences, 8(2), 261-272.

https://doi.org/10.31015/jaefs.2024.2.3

Submission Date: *February 21, 2024*

Acceptance Date: *April 20, 2024*

Early Pub Date: *May 2, 2024*

Publication Date: *June 29, 2024*

Corresponding Author:

Murat EVCIL

E-mail: muratevc@gmail.com

Available at:
https://dergipark.org.tr/jaefs/issue/84099/1441054

INTRODUCTION

In response to growing ecological concerns over plastic waste and depleting fossil fuel reserves, the shift towards biopolymer-based packaging, particularly in food packaging, has gained momentum (Kanmani & Rhim, 2014). Biopolymers offer a sustainable, biodegradable, and non-toxic alternative for food packaging, enabling the extension of food shelf life without direct contact with the food. The interest in natural additives for edible coatings further highlights this trend (Wang & Rhim, 2015).

The shelf life of food products is influenced by factors such as the food's nature, chemical composition, processing, packaging materials, and storage conditions (Pacheco et al., 2019). Edible films, a key research area, contribute to food safety and sustainability but face challenges due to their inferior water vapor barrier properties compared to synthetic films. To improve this, lipids are added to edible films, though this can reduce the film's strength (Xue et al., 2021). Chitosan, known for its antimicrobial properties, faces limitations in physical properties, which can be enhanced by incorporating natural antioxidants and antibacterial agents like essential oils (EOs). Essential oils, derived from natural plant sources, are celebrated for their pronounced antibacterial and antioxidant properties.

Their inclusion in chitosan films markedly improves the antibacterial, antioxidant capabilities, water solubility, and vapor-permeability of the films (T. Liu, Wang, Chi, Tan, & Liu, 2020).

Pomegranate (*Punica granatum* L.), a fruit with a rich historical consumption for its nutritional and medicinal value, continues to draw scientific interest due to its bioactive components and health-promoting benefits. The seed oil of pomegranate, a by-product of the juice manufacturing process, is a significant source of punicic acid, a fatty acid with known health benefits, including antimicrobial, antioxidant, and anticancer properties (Paul & Radhakrishnan, 2020).

Pomegranate seed oil (PSO), rich in beneficial fatty acids and antioxidants, is underutilized in chitosan films. Despite the extensive investigation into the chemical, physical, structural, and biological properties of chitosan films infused with EOs, studies focusing on chitosan composite films containing PSO are sparse. This research utilized cold-pressed PSO, reputed for its superior fatty acid profile and physicochemical properties, such as low peroxide value, high phenolic content, and enhanced aroma profile (Khoddami, Man, & Roberts, 2014). The study aimed to evaluate the antibacterial efficacy of PSO and hypothesized that its addition to chitosan films would improve their antimicrobial properties. The primary objective was to characterize the physicochemical properties of the CH-control and CHPS films using SEM, FTIR, XRD, and UV-visible analyses while examining changes in their mechanical characteristics and antimicrobial activity.

MATERIALS AND METHODS

Materials Acquisition

Methanol, ethanol, and acetic acid were obtained from Carlo Erba. Chitosan with a low molecular weight and 75% deacetylation level were procured from Sigma-Aldrich and used as received. Pomegranate seed oil was purchased from Dnl, a local company in Turkey, that produces oil using the cold pressing method. All experimental procedures were conducted in an oxygen-free nitrogen environment, employing solvents that were not subjected to any purification process.

Film Characterization Techniques

For film analysis, an Agilent 630 device was utilized to capture FT-IR spectra, while the phenolic composition of pomegranate seed essential oil was determined using an Agilent 6890N GC (GC-MS). The surface morphology of the CH and CHPS films and their crystalline structures were examined using an SEM FEI-Quanta-250-FEG and a Bruker-AXS-D8 Advance X-ray diffractometer, respectively. Film thickness was measured in micrometers using an Insize digital micrometer, whereas thermal properties and elemental composition were assessed with a TGA Shimadzu DSC-60 and through elemental analysis, respectively.

Essential Oils Volatile Components Analysis via GC-MS

The analysis of the volatile components in the essential oils (EOs) incorporated into CH-PSO films was performed using GC–MS. The system consisted of an Agilent 6890N GC paired with a 5973 Network mass selective detector, equipped with a 30m, 0.25mm i.d., 0.25 µm film-coated Stabilwax®-DA capillary column by Restek. The EOs were diluted in acetone, with 1 µL injected at a 250 °C injector temperature with a 10:1 split ratio. The temperature program started at 60 °C, increased to 200 °C at 8 °C/min, held for 1 min, then increased to 240 °C at 20 °C/min, and held for 3.5 min. Helium served as the carrier gas at a flow rate of 1.0 mL/min. Mass spectrometry settings included an ion source temperature of 230 °C, electron energy of 70 eV, multiplier voltage of 1447 V, GC/MS transfer line temperature of 250 °C, and a scan range from 33 to 650 mass units. Compound identification was based on comparisons with existing spectral libraries.

Preparation of Chitosan-Based Films

The film formation process was executed using the solvent casting technique as outlined in prior studies (Mouhoub et al., 2022). In summary, chitosan at a concentration of 2% (w/v) was dissolved in 1% acetic acid with continuous agitation. Following the integration of glycerol (as a plasticizer) and Tween 80 (as an emulsifier), essential oils were added at a 2% (v/v) concentration. These components were then uniformly blended at 40 °C for 10 minutes utilizing an ultrasonic cleaner (Wisd WiseClean WUC A22H). Afterward, 3 mL of this blended mixture was evenly spread over a 5-cm diameter plastic mold and subjected to drying at 40 °C for 48 hours within an oven. The resultant films were then prepared for subsequent evaluations. A film devoid of essential oil served as the control group, whereas a film embedded with a mixture of essential oil (0.2% v/v for each type) was employed to assess the synergistic effects of three films with essential oil under investigation. Various concentrations of pomegranate seed oil (2.5%, 5.0%, and 7.5%) were also integrated into the film solutions. A formulation excluding both pomegranate seed oil and Tween 80 was designated as the baseline control. The produced chitosan films were stored in Petri dishes at 4 °C until further examination (Figure 1).

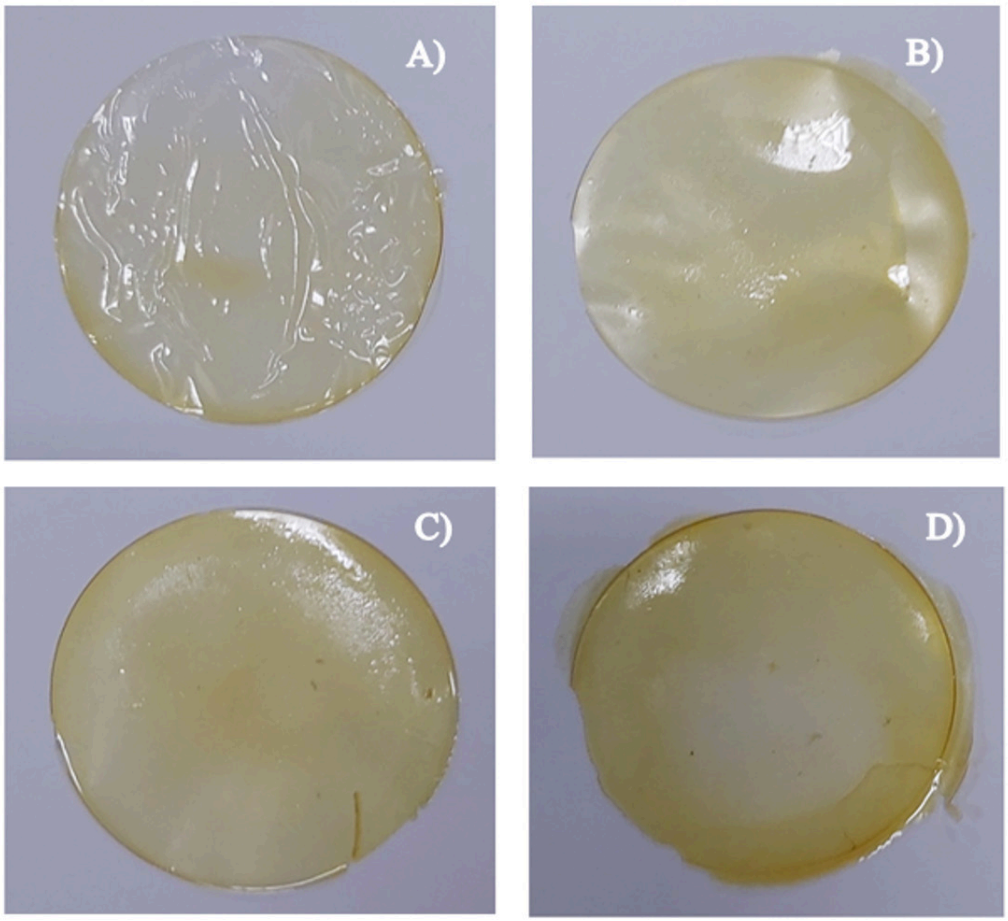

Figure 1. Photographs of CH control (A), CHPS-2.5% (B) , CHPS-5.0% (C), CHPS-7.5% (D).

Physical properties of films

Thickness of the Films

The thickness of films was measured with a micrometer with an ac-curacy of 1 µm and thickness. Measurements were taken at five distinct points for each film using a digital micrometer (Insize, China). The average value was then calculated and used for characterization.

Moisture Content (MC)

Moisture content of film samples (2.4x2.4 cm^2) was determined by measuring their mass loss after oven drying at 105 °C for 24 h. The moisture content was calculated as follows (Eq. 1):

Moisture content: $(W_1\text{-}W_2)/W_1$ x 100 (1)

where W_1 is the initial weight of the film and W_2 is its final weight post-drying.

Solubility of Films in Water

Pieces of film 2.4 x 2.4 cm^2, were cut from each film and weighed. The solubility in water of the different blend films was measured from immersion assays under constant agitation in 50 mL of distilled water for 24 h at 25 °C. The remaining pieces of film after immersion were dried at 105 °C in oven (a Pol-Eko-Aparture son 53,115) to constant weight (final dry weight). The initial dry weight was determined by thermal processing at 105 °C to constant weight. Solubility in water (%) was calculated as follows (Eq. 2):

Water solubility (%) = $((W_0\text{-}W_f)/W_0) \times 100$ (2)

Where W_0 is the initial dry weight of the film, and W_f represents the weight of the residual, non-dissolved film after immersion.

Optical properties

Optical transmittance

The transparency of prepared films was measured at selected wavelengths (250–500 nm) using a Lambda 40 UV/Vis spectrophotometer (Shimadzu-1900). Filmsamples was cut into a rectangle piece and attached to a quartz cell and placed in a spectrophotometer test cell directly, and air was used as reference. Measurements were performed at least in three replicates.Tthe results were reported as the samples' percent transmittance (%T), calculated as follows (Eq. 3):

$$\%T=10^{-A} \times 100. \quad (3)$$

As a reference, an empty cuvette, or air, was utilized. Optical transmittance examination of the films was performed with a UV spectrophotometer (Shimadzu -1900) in the 250–500 nm range (Bajić et al., 2019).

Scanning electron microscopy (SEM)

Surface as well as cross-sectional morphologies of the CH-control and CHPSs films were investigated using FEI Quanta 250 FEG model SEM. The film samples were cut into small pieces, then mounted on aluminum stubs with adhesive tape.

X-ray diffraction (XRD)

The crystalline characteristics of CHPSs were assessed using XRD with Ni-filtered Cu Kα radiation, scanning in the 2θ range from 0° to 60°. The X-ray analyses were carried out on CH powder, CH control and CHPS-7.5% films.

Antimicrobial Properties

The antimicrobial efficacy of CHPS films containing 2.5% to 7.5% concentrations was assessed against foodborne pathogens, including the Gram-negative bacteria *Escherichia coli* ATCC 25922 (*E. coli*) and the Gram-positive bacteria *Staphylococcus aureus* ATCC 25923 (*S. aureus*), along with the fungus *Candida albicans*, using the disc diffusion method. Cultivation of these microorganisms was performed under optimal conditions in suitable media at 37°C. Mueller-Hinton agar, provided by Merck, served as the testing medium for the antimicrobial analysis. Microbial solutions were standardized to match the McFarland 0.5 turbidity standard, equating to 1.5x108 CFU/mL. Sterile discs were saturated with the CHPS films at varying concentrations (2.5%, 5.0%, and 7.5%) and pure chitosan for comparison. These discs were then methodically placed on Mueller-Hinton agar plates inoculated with each microbe. The agar plates were incubated at 37°C for 24 hours to allow for interaction between the microbes and the films' active components. Following the incubation, the zones of inhibition around each disc were observed and measured in millimeters using a digital caliper to quantify the antimicrobial effect.

RESULTS AND DISCUSSION

Gas Chromatography-Mass Spectrometer (GC-MS) analysis of Pomegranate Seed Essential Oil profiles

The volatile profiles of pomegranate seed essential oil were ascertained using Agilent 6890N GC (GC-MS). Table 1 presents the results of compound determinations from GC-MS analyses.

Table 1. Chemical Constituents of Pomegranate (*Punica granatum* L.) Seed Essential Oil

Chemical constituents	Result (%)	Chemical constituents	Result (%)
Butyric acid (C4:0)	0,11	Linoleic acid (C18:2)	18,72
Caproic acid (C6:0)	0,12	Linolenic acid (C18:3)	0,36
Caprylic acid (C8:0)	-	Arachidic acid (C20:0)	0,23
Capric acid (C10:0)	-	Eicosenoic acid (C20:1)	0,25
Lauric acid (C12:9)	-	Eicosadienoic acid (C20:2)	-
Myristic acid (C14:0)	0,03	Behenic acid (C22:0)	0,29
Palmitic acid (C16:0)	8,40	Erucic acid (C22:1)	-
Palmitoleic acid (C16:1)	0,06	docosadienoic acid (C22:2)	-
Margaric acid (C17:0)	-	Tricosanoic acid (C23:0)	15,93
Heptadecenoic acid (C17:1)	0,09	Lignoceric acid (C24:0)	2,55
Stearic acid (C18:0)	2,98	Nervonic acid (C24:1)	-
Oleic acid (C18:1)	49,88		

Analysis of Fourier-Transform Infrared Spectroscopy

FT-IR analysis was utilized to elucidate the molecular interactions between chitosan and pomegranate seed oil (PSO) within the films. The FTIR spectra depicted in Figure 2 highlight the differences between chitosan films with and without PSO incorporation. For the chitosan control film, notable features include a wide band spanning from 4000 to 3000 cm^{-1}indicative of O–H bond stretching; peaks at 2929 cm^{-1} and 2858 cm^{-1} representing symmetric and asymmetric CH2 vibrations, respectively; and a peak at 1546 cm^{-1} associated with N–H bending of amide II. The presence of residual N-acetyl groups in chitosan is confirmed by bands around 1643 cm^{-1}, attributable to C=O stretching of amide I, while the band at 1148 cm^{1} suggests asymmetric stretching of the C–O–C bridge.

In films containing PSO, the FTIR spectrum reveals distinctive bands: a peak at 3499 cm^{-1} is linked to NH stretching, and the peak at 3011 cm^{-1} to C-H vibrations of cis-alkene. The band at 1744 cm^{-1} corresponds to C-O stretching vibrations of carbonyl groups in triacylglycerols. The spectrum also shows a band at 2922 cm^{-1} for C-H stretching of methylene and -CH2 groups in lipids, and a sharp peak at 2851 cm^{-1}, typically associated with terminal -CH3 groups. Notably, the spectrum features a strong absorption band at 1635 cm^{-1}, characteristic of amide I β-sheet structures, along with bands at 984 $cm^{-1}$and 760 cm^{-1}indicative of amide III β-sheets and CH bending, respectively (Adiba et al., 2023).

With the addition of PSO to chitosan films, shifts in spectral peaks were observed, including from 3313 cm^{-1} to 3373 cm^{-1} for NH and OH stretching vibrations, and from 1546 cm^{-1} to 1554 cm^{-1} indicating changes in NH bending. A shift from 1379 cm^{-1} to 1364 cm^{-1} in CN stretching vibration was noted, alongside a significant reduction in peak intensity. The peak at 2858 cm^{-1} divided into two at 2851 cm^{-1} and 2918 cm^{-1}, reflecting symmetric and asymmetric CH vibrations (T. Liu, Liu, Gong, Chi, & Ma, 2021). Additionally, the intensity of the peak at 1010 cm^{-1}, corresponding to C–O–C stretching, decreased significantly upon PSO addition, likely due to hydrogen bonding interactions between polyphenols' hydroxyl groups and chitosan's hydroxyl and amino groups (T. Liu et al., 2021; Nguyen & Bui, 2020).

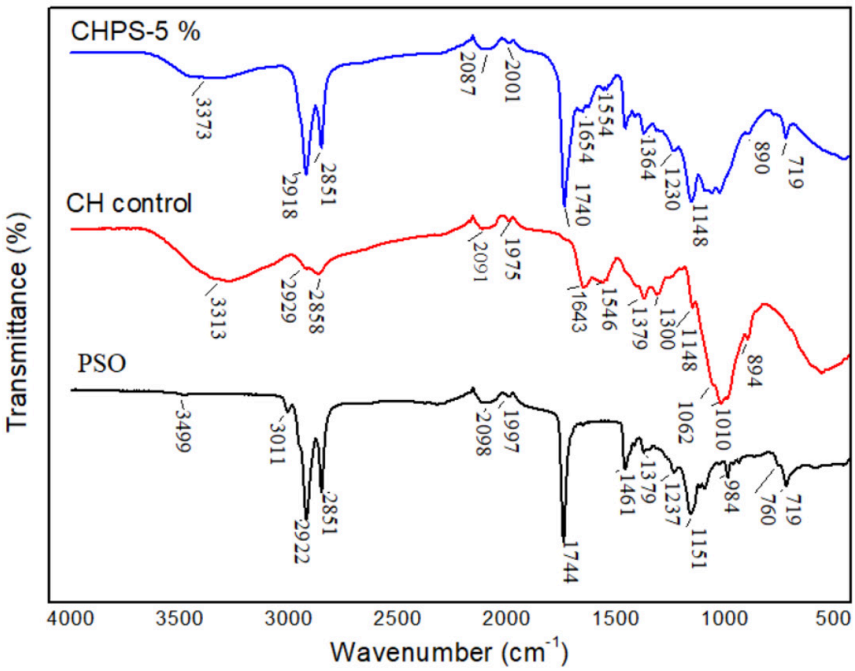

Figure 2. FT-IR Spectra of CH, CH control and CHPS

Scanning Electron Microscopy Analysis

Scanning Electron Microscopy (SEM) analysis provided insights into the surface morphology of CHPS films with PSO concentrations ranging from 2.5% to 7.5% (v/v), as illustrated in Figure 3. The SEM images revealed that the CHPS films exhibited a rough and non-uniform surface texture. Specifically, the chitosan films integrated with PSO displayed significant variations in microstructure, particularly at higher PSO concentrations, leading to a heterogeneous appearance due to the incorporation of oil droplets within the polysaccharide matrix. Notably, these oil droplets deviated from the typical spherical shape found in oil/water emulsions, possibly due to the chitosan matrix's tensile forces during the drying process.

Comparatively, chitosan films without PSO addition were characterized by a smooth, flat surface without any visible cracks, indicating uniformity. The introduction of PSO, however, altered the film's microstructure markedly, embedding oil droplets unevenly throughout the chitosan network. This disruption increased with the PSO concentration, making the droplets more prominent and less spherical, suggesting an interaction with the chitosan framework.

Reference to a study by Hafsa, J., et al.(2015) (Hafsa et al., 2016) highlighted that chitosan films impregnated with Eucalyptus globulus essential oil nanoemulsion at varying concentrations (0-4% v/v) maintained a smooth and continuous structure at lower oil concentrations. Yet, as the oil nanoemulsion concentration escalated, the films exhibited an increase in oil droplet presence, closely integrated within the polymer matrix. The phenomenon of oil droplet enlargement with rising PSO content was also observed, with the largest droplets becoming visible at higher magnifications in films with the highest PSO levels. This trend was attributed to the increased likelihood of droplet collisions and subsequent coalescence in higher lipid-content emulsions (McClements, 2004).

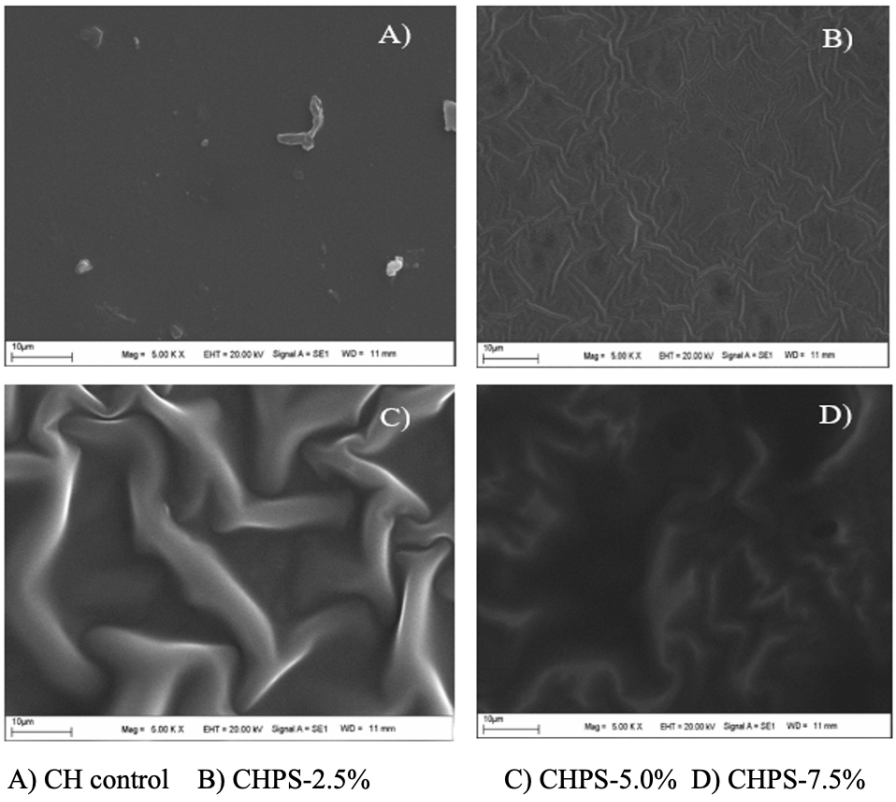

Figure 3. SEM Micrographs of CH control and CHPS-2.5-7.5 % films.

X-Ray diffraction analysis (XRD) patterns of CHPSs

XRD analysis was conducted to investigate the crystallinity within the film components. The XRD patterns for CH powder, the CH control film (CH/glycerol), and CHPS-7.5% films are shown in Figure 4. CH powder is observed to be semi-crystalline, displaying two primary peaks at 2θ=14° and 20° (Evcil & Karakaplan, 2022; J. Liu et al., 2016), which are indicative of inter- and intra-molecular hydrogen bonding facilitated by the presence of free amino groups.

The XRD pattern for the mixture without PSO reveals its crystallinity with a distinctive peak at 20.88°, suggesting that the CH/Gly films have a quasi-amorphous form with limited crystallization, likely reflecting the semi-crystalline nature of chitosan. This result implies that the strong interactions, such as hydrogen bonding and ionic interaction between glycerol and chitosan, might be disrupted in the blend films' matrix, leading to a more organized packing of chitosan molecules and formation of a regular crystalline structure (Ghaffari, Navaee, Oskoui, Bayati, & Rafiee-Tehrani, 2007).

When PSO is added to the CH/Gly blend films, there is a slight shift in the peak position to 20.22° in the XRD pattern, but the peak intensity decreases compared to the CH/Gly films. This suggests that PSO disperses at the molecular level within the biopolymer matrix, likely forming interactions with glycerol and chitosan's functional groups. Therefore, it can be concluded that PSO incorporation does not significantly alter the amorphous structure of the blend films.

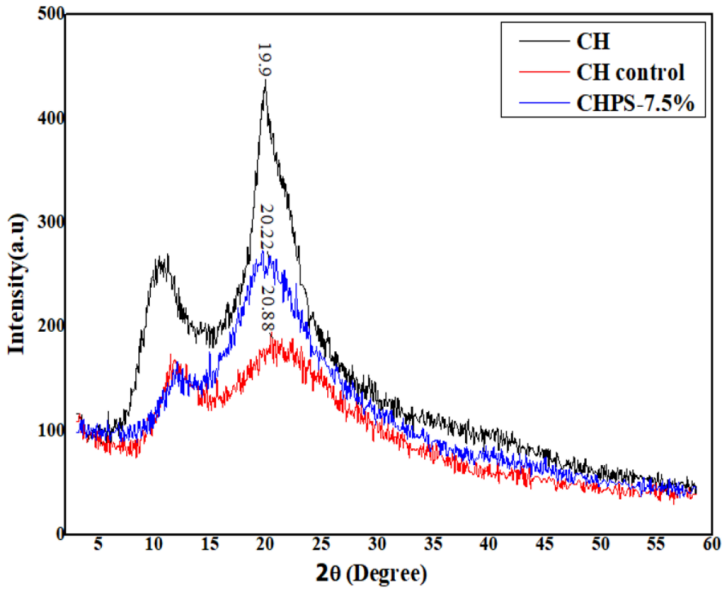

Figure 4. XRD of CH, CH control and CHPS-7.5%

Thickness

Film thickness is a crucial parameter affecting the film's physical and mechanical characteristics, such as its barrier properties against water, gases, and moisture, along with its tensile strength and resistance to impact (Hosseini, Ghaderi, & Gómez-Guillén, 2021). As presented in Table 2, the thickness measurements for films comprising chitosan-control (CH control), CHPS-2.5%, CHPS-5.0%, and CHPS-7.5% were recorded at 0.051 mm, 0.30mm, 0.60 mm, and 0.66 mm, respectively. These findings align with those from previous research (Haghighi et al., 2019;Li et al., 2019), which suggest that the observed increase in film thickness can be attributed to the addition of solid content within the film matrix. An observed increase in the film network's density is attributed to the integration of various chemical compounds found in essential oils, which in turn affects the arrangement of chitosan chains (Khezrian & Shahbazi, 2018).

Water Solubility

Table 2 displays the solubility in water for both the CH-control film and the chitosan films enhanced with PSO. A decline in the solubility of the films in water was observed, decreasing from 11.08% to 8.11%, as the inclusion of PSO was raised from 2.5% in the CHPS-2.5% film to 7.5% in the CHPS-7.5% film. The decrease in moisture content due to the non-polar nature of the essential oil used in our research parallels previous findings with lemon essential oil (Bof, Jiménez, Locaso, García, & Chiralt, 2016). This effect is likely attributable to the covalent bonding between the chitosan polymer and the functional groups within the oil as PSO is amalgamated into the chitosan films. Consequently, this diminishes the availability of chitosan's hydroxyl and free amine groups to interact with water, thereby reducing water interaction within the polysaccharide. The diminished water affinity with chitosan films further impacts their solubility in water significantly. The resilience of the chitosan film network was highlighted by their near intact state after 24 hours of immersion in water. A decrease in dry mass of the films indicates a degree of solubility. The solubility rate of the chitosan control film in water corroborates with prior studies (27.35%) (K., G., Banat, Show, & Cocoletzi, 2019), indicating a reduction from approximately 28.1% for the neat chitosan or CH-control film to about 8.11% for the CHPS-7.5% films, thereby marking a significant decrease as the proportion of PSO in chitosan escalates.

Table 2. Thickness, moisture content and water solubility of films

Samples	Thickness (mm)	Water Solubility (%)	Moisture Content (%)
CH control	0.051	28.1	21.25
CHPS-2.5%	0.30	11.08	21.78
CHPS-5.0%	0.60	10.03	20.72
CHPS-7.5%	0.66	8.11	16.76

Moisture Content (MC%)

The introduction of phenolic compounds resulted in a significant reduction ($p < 0.05$) in the moisture content of the films, as detailed in Table 2, when compared to the control sample. This reduction can be linked to enhanced molecular interactions and an increase in hydrophobic properties. Additionally, the moisture content in these edible films was considerably influenced by the specific type or characteristics of the phenolic compounds utilized, with the films infused with PSO exhibiting the lowest moisture content. This finding aligns with the results of previous studies, such as those conducted by Hafsa, J., et al., indicating similar outcomes (Hafsa et al., 2016).

Optical Transmittance

Characteristics related to optical transmittance, including color and clarity, are vital for determining the acceptability and visual appeal of the film to end-users. Transparency, an essential measure for evaluating the clarity of the film, indicates that a higher transparency value corresponds to reduced clarity of the film. The transparency levels of the films, both CH-control and those containing CHPS, are depicted in Figure 5. Among all films tested, the CH-control film exhibited the highest light transmittance, at 66.3%. The inclusion of plasticizers and PSO resulted in a notable decrease ($p < 0.05$) in optical transmittance from the CHPS-2.5% to the CHPS-7.5% films, with the CHPS-5.0% and CHPS-7.5% films demonstrating lower light transmission. The presence of Gly and PSO in the films leads to the creation of structures that contain oil or water droplets, which disrupt light transmittance and increase light scattering at the droplet boundaries. These observations indicate that PSO and Gly can effectively block the transmission of ultraviolet rays through these edible films. Furthermore, the films containing PSO showed reduced transparency due to the colorful constituents of PSO. From a commercial perspective, these composite films enriched with PSOs can obstruct the passage of UV rays, thereby providing enhanced protection for light-sensitive food products against oxidation and other external factors that could damage the food (Mohammadi, Mirabzadeh, Shahvalizadeh, & Hamishehkar, 2020).

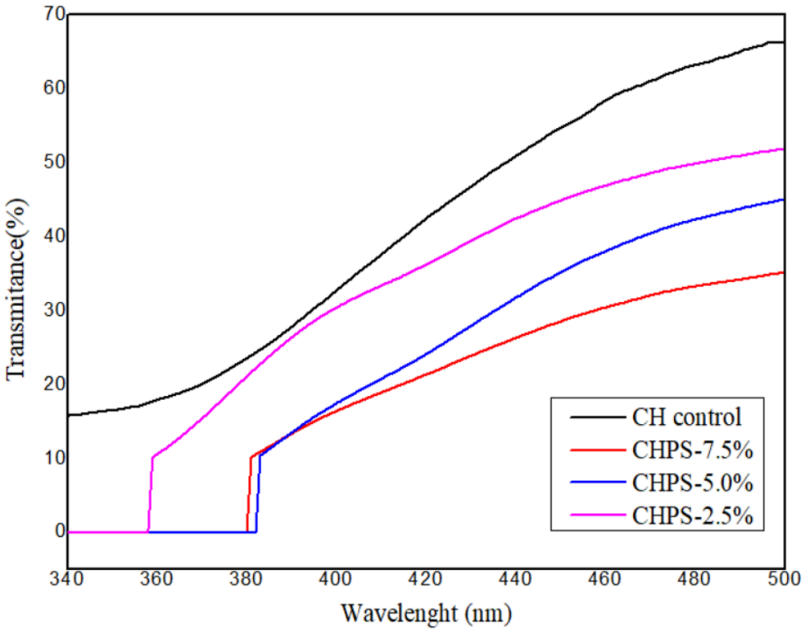

Figure 5. The light transmittance of CH control and CHPSs in the UV–vis light region

Antimicrobial Properties

The antimicrobial effects of CHPS-2.5-7.5% films prepared with three different concentrations were examined on food pathogens and the fungus *C. albicans* using the disc diffusion method. Measurements, revealed that the inhibition zones formed due to the antimicrobial effect of CHPS-2.5-7.5% films were significantly larger compared to chitosan. When it comes to inhibiting the growth of Gram-negative *E. coli*, it seems that various concentrations of CHPS-2.5-7.5 are more effective than the control. When compared to the control, the effect of the various concentrations of CHPS-2.5-7.5 on the other strains that were utilised in the application was found to be quite insignificant(Table 1). Among the microorganisms that were utilised in the application, gram-negative *E. coli* was one of the microorganisms that was

found to be considerably successful in reducing the growth of CHPS-2.5-7.5 percent films. The presence of inhibitory zones gives the impression that it is successful in suppressing the growth of other strains, despite the fact that its effect on other strains is insignificant in comparison to the control.Herbal extracts are compounds rich in phenols and flavonoids. These compounds exhibit bioactive properties, including antimicrobial and antioxidant activities (Rauf et al., 2019)"id":"ITEM-1","issued":{"date-parts":[["2019","8"]]},"page":"108999","title":"Proanthocyanidins: A comprehensive review","type":"article-journal","volume":"116"},"uris":["http://www.mendeley.com/documents/?uuid=8374df55-21c9-422c-9892-dde1e1ac2c8e"]}],"mendeley":{"formattedCitation":"(Rauf et al., 2019. In the (GC-MS) profile (Table 1), shows high concentrations of phenolic and flavonoid compounds, including protocatechuic acid, chlorogenic acid, vanillin, and isoquercitrin. The presence of these compounds in the structure of the films shows that they are effective in antimicrobial activity (Eroglu & Girgin, 2021). Phenolic and flavonoid compounds found in plant extracts increase the ROS level in microorganisms. These bioactive compounds act by negatively interfering with the synthesis of important molecules such as biofilm, glucosamine, and proteins. In addition, these compounds in the extract show antimicrobial effects by causing structural and functional disruption of cell membranes, inhibition of important enzymes such as DNA gyrase and protein kinase, and inhibition of dehydratase and type III secretion inactivation mechanisms (Rempe, Burris, Lenaghan, & Stewart, 2017;Silva et al., 2021; Wali et al., 2020;Yang et al., 2022).

Table 3. Measurement results of inhibition zones formed due to the antimicrobial effects of CHPS-2.5-7.5% and control (chitosan) films on food pathogens and fungus C. *albicans* for 24 hours using the Disc Diffusion method

			Films in different concentrations Measured Inhibition Zones (mm)			
			Control (Chitosan)	0.25 μg mL^{-1}	0.50 μg mL^{-1}	1.00 μg mL^{-1}
Microorganism	Bacteria	***E. coli***	7.00	8.00	8.00	8.00
		S. aureus	9.00	8.00	8.00	8.00
	Fungus	***C. albicans***	9.00	8.00	8.00	8.00

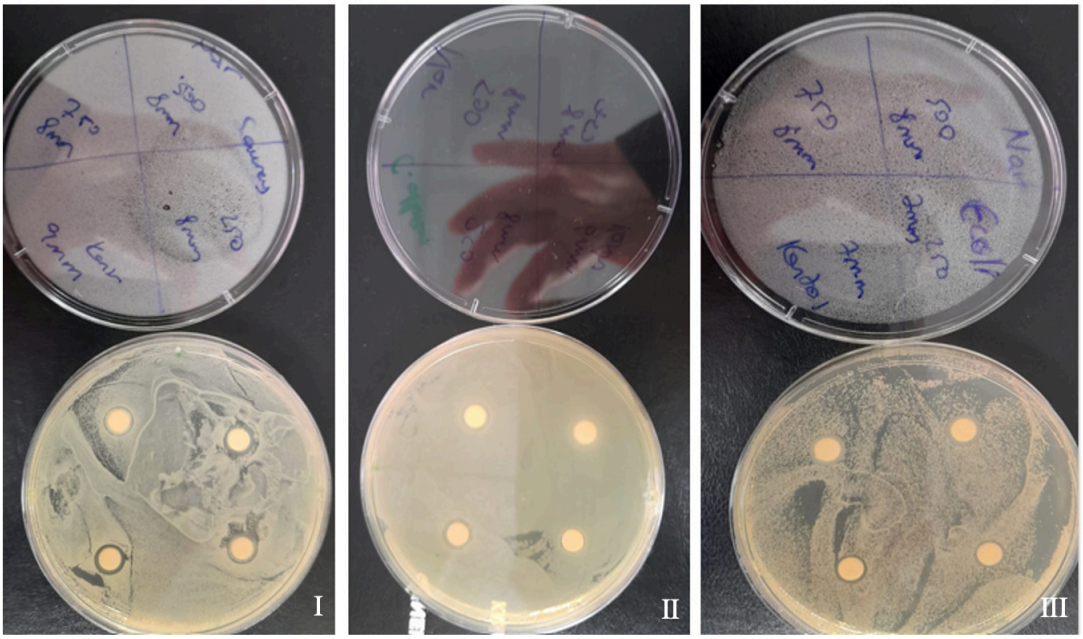

Figure 6. Inhibition zones formed as a result of the antimicrobial effects of CHPS-2.5-7.5% films on food pathogens and fungi through the Disc Diffusion method; Inhibition zones formed as a result of the antimicrobial effects of 0.25, 0.50, and 1.00 concentrations of CHPS-2.5-7.5% films on (I) *S. aureus*, (II) *C. albicans*, and (III) *E. coli*

CONCLUSION

In summary, this research has successfully integrated pomegranate seed essential oil into chitosan films and assessed their characteristics. X-ray diffraction analysis demonstrated the semi-crystalline nature of the films, with the inclusion of PSO enhancing their solubility. An increase in the concentration of PSO led to a reduction in the moisture content of the films. It was observed that with a higher binding ratio of PSO to chitosan, the thickness of the films increased, while their water solubility and moisture content decreased. The antimicrobial capabilities of the films were also investigated, revealing that chitosan films infused with PSO exhibited antimicrobial properties. These results indicate that chitosan films containing PSO could serve as a viable alternative to synthetic polymers in food coating and packaging sectors. Future research should focus on exploring the potential uses of these films in a variety of applications.

Compliance with Ethical Standards

Peer-review

Externally peer-reviewed.

Conflict of interest

The author declared no potential conflicts of interest with respect to the research, authorship, and/or publication of this article.

Author contribution

The author read and approved the final manuscript. The author verifies that the Text, Figures, and Tables are original and that they have not been published before.

Funding

No financial support was received for this study.

Data availability

Not applicable.

Consent to participate

Not applicable.

Consent for publication

Not applicable.

REFERENCES

Adiba, A., Razouk, R., Haddioui, A., Ouaabou, R., Hamdani, A., Kouighat, M., & Hssaini, L. (2023). FTIR spectroscopy-based lipochemical fingerprints involved in pomegranate response to water stress. *Heliyon*, *9*(6), e16687. https://doi.org/10.1016/j.heliyon.2023.e16687

Bajić, M., Ročnik, T., Oberlintner, A., Scognamiglio, F., Novak, U., & Likozar, B. (2019). Natural plant extracts as active components in chitosan-based films: A comparative study. *Food Packaging and Shelf Life*, *21*, 100365. https://doi.org/10.1016/j.fpsl.2019.100365

Bof, M. J., Jiménez, A., Locaso, D. E., García, M. A., & Chiralt, A. (2016). Grapefruit Seed Extract and Lemon Essential Oil as Active Agents in Corn Starch–Chitosan Blend Films. *Food and Bioprocess Technology*, *9*(12), 2033–2045. https://doi.org/10.1007/s11947-016-1789-8

Eroglu, E., & Girgin, S. N. (2021). A unique phenolic extraction method from olive oil macerate of Hypericum perforatum using DMSO: Assessment of in vitro anticancer activity, LC-MS/MS profile, total phenolic content and antioxidant capacity. *South African Journal of Botany*, *139*, 6–11. https://doi.org/10.1016/j.sajb.2021.01.015

Evcil, M., & Karakaplan, M. (2022). Salicylaldehydediol Grafted onto Chitosan: Characterization and Their Film Properties. *Journal of the Turkish Chemical Society Section A: Chemistry*, *9*(3), 879–888. https://doi.org/10.18596/jotcsa.1084225

Ghaffari, A., Navaee, K., Oskoui, M., Bayati, K., & Rafiee-Tehrani, M. (2007). Preparation and characterization of free mixed-film of pectin/chitosan/Eudragit® RS intended for sigmoidal drug delivery. *European Journal of Pharmaceutics and Biopharmaceutics*, *67*(1), 175–186. https://doi.org/10.1016/j.ejpb.2007.01.013

Hafsa, J., Smach, M. ali, Ben Khedher, M. R., Charfeddine, B., Limem, K., Majdoub, H., & Rouatbi, S. (2016). Physical, antioxidant and antimicrobial properties of chitosan films containing Eucalyptus globulus essential oil. *LWT - Food Science and Technology*, *68*, 356–364. https://doi.org/10.1016/j.lwt.2015.12.050

Haghighi, H., Biard, S., Bigi, F., De Leo, R., Bedin, E., Pfeifer, F., … Pulvirenti, A. (2019). Comprehensive characterization of active chitosan-gelatin blend films enriched with different essential oils. *Food Hydrocolloids*, *95*, 33–42. https://doi.org/10.1016/j.foodhyd.2019.04.019

Hosseini, S. F., Ghaderi, J., & Gómez-Guillén, M. C. (2021). trans-Cinnamaldehyde-doped quadripartite biopolymeric films: Rheological behavior of film-forming solutions and biofunctional performance of films. *Food Hydrocolloids*,

112, 106339. https://doi.org/10.1016/j.foodhyd.2020.106339

K., R., G., B., Banat, F., Show, P. L., & Cocoletzi, H. H. (2019). Mango leaf extract incorporated chitosan antioxidant film for active food packaging. *International Journal of Biological Macromolecules*, *126*, 1234–1243. https://doi.org/10.1016/j.ijbiomac.2018.12.196

Kanmani, P., & Rhim, J.-W. (2014). Properties and characterization of bionanocomposite films prepared with various biopolymers and ZnO nanoparticles. *Carbohydrate Polymers*, *106*, 190–199. https://doi.org/10.1016/j.carbpol.2014.02.007

Khezrian, A., & Shahbazi, Y. (2018). Application of nanocompostie chitosan and carboxymethyl cellulose films containing natural preservative compounds in minced camel's meat. *International Journal of Biological Macromolecules*, *106*, 1146–1158. https://doi.org/10.1016/j.ijbiomac.2017.08.117

Khoddami, A., Man, Y. B. C., & Roberts, T. H. (2014). Physico-chemical properties and fatty acid profile of seed oils from pomegranate (Punica granatum L.) extracted by cold pressing. *European Journal of Lipid Science and Technology*, *116*(5), 553–562. https://doi.org/10.1002/ejlt.201300416

Li, Z., Lin, S., An, S., Liu, L., Hu, Y., & Wan, L. (2019). Preparation, characterization and anti-aflatoxigenic activity of chitosan packaging films incorporated with turmeric essential oil. *International Journal of Biological Macromolecules*, *131*, 420–434. https://doi.org/10.1016/j.ijbiomac.2019.02.169

Liu, J., Meng, C., Yan, Y., Shan, Y., Kan, J., & Jin, C. (2016). Protocatechuic acid grafted onto chitosan: Characterization and antioxidant activity. *International Journal of Biological Macromolecules*, *89*, 518–526. https://doi.org/10.1016/j.ijbiomac.2016.04.089

Liu, T., Liu, L., Gong, X., Chi, F., & Ma, Z. (2021). Fabrication and comparison of active films from chitosan incorporating different spice extracts for shelf life extension of refrigerated pork. *LWT*, *135*, 110181. https://doi.org/10.1016/j.lwt.2020.110181

Liu, T., Wang, J., Chi, F., Tan, Z., & Liu, L. (2020). Development and Characterization of Novel Active Chitosan Films Containing Fennel and Peppermint Essential Oils. *Coatings*, *10*(10), 936. https://doi.org/10.3390/coatings10100936

McClements, D. J. (2004). *Food Emulsions*. https://doi.org/10.1201/9781420039436

Mohammadi, M., Mirabzadeh, S., Shahvalizadeh, R., & Hamishehkar, H. (2020). Development of novel active packaging films based on whey protein isolate incorporated with chitosan nanofiber and nano-formulated cinnamon oil. *International Journal of Biological Macromolecules*, *149*, 11–20. https://doi.org/10.1016/j.ijbiomac.2020.01.083

Mouhoub, A., Raouan, S. E., Guendouz, A., El Alaoui-Talibi, Z., Koraichi, S. I., El Abed, S., … El Modafar, C. (2022). Antiadhesion effect of the chitosan-based film incorporated with essential oils against foodborne bacteria. *Industrial Crops and Products*, *189*, 115742. https://doi.org/10.1016/j.indcrop.2022.115742

Nguyen, L. T. T., Nguyen, T. T., Nguyen, H. N., & Bui, Q. T. P. (2020). Simultaneous determination of active compounds in Piper betle Linn. leaf extract and effect of extracting solvents on bioactivity. *Engineering Reports*, *2*(10). https://doi.org/10.1002/eng2.12246

Pacheco, N., Naal-Ek, M. G., Ayora-Talavera, T., Shirai, K., Román-Guerrero, A., Fabela-Morón, M. F., & Cuevas-Bernardino, J. C. (2019). Effect of bio-chemical chitosan and gallic acid into rheology and physicochemical properties of ternary edible films. *International Journal of Biological Macromolecules*, *125*, 149–158. https://doi.org/10.1016/j.ijbiomac.2018.12.060

Paul, A., & Radhakrishnan, M. (2020). Pomegranate seed oil in food industry: Extraction, characterization, and applications. *Trends in Food Science & Technology*, *105*, 273–283. https://doi.org/10.1016/j.tifs.2020.09.014

Rauf, A., Imran, M., Abu-Izneid, T., Iahtisham-Ul-Haq, Patel, S., Pan, X., … Rasul Suleria, H. A. (2019). Proanthocyanidins: A comprehensive review. *Biomedicine & Pharmacotherapy*, *116*, 108999. https://doi.org/10.1016/j.biopha.2019.108999

Rempe, C. S., Burris, K. P., Lenaghan, S. C., & Stewart, C. N. (2017). The Potential of Systems Biology to Discover Antibacterial Mechanisms of Plant Phenolics. *Frontiers in Microbiology*, *8*. https://doi.org/10.3389/fmicb.2017.00422

Silva, A., Silva, V., Igrejas, G., Gaivão, I., Aires, A., Klibi, N., … Poeta, P. (2021). Valorization of Winemaking By-Products as a Novel Source of Antibacterial Properties: New Strategies to Fight Antibiotic Resistance. *Molecules*, *26*(8), 2331. https://doi.org/10.3390/molecules26082331

Wali, A. F., Al Dhaheri, Y., Ramakrishna Pillai, J., Mushtaq, A., Rao, P. G. M., Rabbani, S. A., … Farraj, D. A. Al. (2020). LC-MS Phytochemical Screening, In Vitro Antioxidant, Antimicrobial and Anticancer Activity of Microalgae Nannochloropsis oculata Extract. *Separations*, *7*(4), 54. https://doi.org/10.3390/separations7040054

Wang, L.-F., & Rhim, J.-W. (2015). Preparation and application of agar/alginate/collagen ternary blend functional food packaging films. *International Journal of Biological Macromolecules*, *80*, 460–468. https://doi.org/10.1016/j.ijbiomac.2015.07.007

Xue, F., Zhao, M., Liu, X., Chu, R., Qiao, Z., Li, C., & Adhikari, B. (2021). Physicochemical properties of chitosan/zein/essential oil emulsion-based active films functionalized by polyphenols. *Future Foods*, *3*, 100033. https://doi.org/10.1016/j.fufo.2021.100033

Yang, Z., Li, L., Chen, C., Zhang, Y., Yang, Y., Zhang, P., & Bao, G. (2022). Chemical composition and antibacterial activity of 12 medicinal plant ethyl acetate extracts using LC–MS feature-based molecular networking. *Phytochemical Analysis*, *33*(3), 473–489. https://doi.org/10.1002/pca.3103